chemosensors

MDPI

Article

Commercial Screen-Printed Electrodes as pH Voltammetric Sensors

Alex Campos [1], Luna Ipharraguerre [1], Clara Pérez-Ràfols [1,2,*], Núria Serrano [1,2,*] and José Manuel Díaz-Cruz [1,2]

[1] Department of Chemical Engineering and Analytical Chemistry, Universitat de Barcelona (UB), Martí i Franquès 1-11, 08028 Barcelona, Spain; josemanuel.diaz@ub.edu (J.M.D.-C.)
[2] Water Research Institute (IdRA), Universitat de Barcelona (UB), Martí i Franquès 1-11, 08028 Barcelona, Spain
* Correspondence: claraperezrafols@ub.edu (C.P.-R.); nuria.serrano@ub.edu (N.S.)

Abstract

The development of miniaturized pH sensors suitable for routine analytical implementation remains a central challenge in electrochemical analysis. Here, a critical assessment of commercial screen-printed electrodes (SPEs) as voltammetric pH sensors is presented, focusing on their electrochemical response, analytical response and practical limitations. Screen-printed carbon electrodes (SPCEs) and screen-printed gold electrodes (SPAuEs) were evaluated under minimal treatment. SPCEs exhibited no intrinsic pH sensitivity, and quinone-based electrochemically deposited layers showed insufficient stability for reliable measurements. In contrast, SPAuEs showed a well-defined pH-dependent response based on the reduction of electrochemically generated gold oxides. After HCl pretreatment, near-to super-Nernstian behaviour (up to 64 mV) was achieved over a wide pH range (2–12). SPAuEs demonstrated excellent inter-electrode reproducibility and good temporal stability, with variations not exceeding ±0.12 pH units. However, repeatability was affected by progressive surface modification, particularly at alkaline pH. This limitation was mitigated by introducing an intermediate regeneration step in acidic medium, which restores a consistent surface state. Accurate pH determinations were achieved across several buffer systems at 0.1 mol L^{-1} ionic strength, whereas lower ionic strengths and chloride ions significantly affected sensor performance. These results demonstrate that a pH-dependent gold oxide response alone does not guarantee reliable pH measurements. Instead, successful implementation of commercial SPAuEs requires appropriate surface conditioning, regeneration procedures and control of matrix effects. By defining these operational requirements and limitations, this work establishes a practical framework for the reliable use of commercial SPAuEs as voltammetric pH sensors.

Keywords: screen-printed electrodes; pH sensing; gold electrodes; voltammetry; miniaturized sensor

Check for updates

Received: 19 October 2026
Revised: 16 November 2026
Accepted: 18 November 2026
Published: 21 November 2026

Copyright: © 2026 by the authors. Licensee MDPI, Basel, Switzerland. This article is an open access article distributed under the terms and conditions of the Creative Commons Attribution (CC BY) license.

1. Introduction

As a key parameter in chemical sciences, pH governs fundamental principles including chemical equilibria and reactivity, acid–base behaviour, electrochemical processes and solubility phenomena. As a result, numerous chemical parameters depend directly on pH, which functions both as a variable that shapes how systems behave and as a parameter that allows one to understand the processes occurring within those systems. Its relevance extends across diverse fields, from environmental monitoring and industrial process control to biomedical research, pharmaceuticals, food production and electrochemistry, where

precise acidity control is essential for ensuring system stability, product performance and reliable analytical interpretation.

Since its introduction in the 1900s, the glass electrode has become the gold standard for pH determination as it provides reliable and accurate pH measurements. Nevertheless, the inherent design of glass electrodes results in bulky, fragile and costly electrodes with limited applicability in certain scenarios [1,2]. In particular, the large dimensions of the conventional glass electrode have prompted the development of alternative pH sensors aimed at achieving miniaturized devices that allow the determination of low-volume samples or local pH changes, as well as pH sensors that are easily adaptable to microfluidic devices. As a result, a wide range of miniaturized pH sensors has been developed for applications as diverse as wearable sensors [3,4], biochemical applications [5], localized pH sensing in bio-electrochemistry and electrocatalysis [6], or microfluidic devices for environmental applications [7].

In this context, screen-printed electrodes (SPEs) offer a particularly attractive platform for miniaturized electrochemical sensing, as they combine the whole electrochemical cell into a small and well-defined area that can be easily adapted to the desired geometry. More importantly, multiple commercial alternatives are available for SPEs based on different materials, thus facilitating its introduction in non-specialized analytical laboratories worldwide.

In terms of sensing material, three main families of potentiometric or amperometric pH sensors have been developed [5]: (i) solid-state ion selective electrodes based on selective membranes that include an ionophore, an ion-exchanger and a polymeric matrix, typically with a plasticizer [4]. In these systems, the ionophore provides ion selectivity, while the polymeric matrix offers mechanical support and regulates ionic diffusion; (ii) metal oxide thin films such as IrO_2, TiO_2, RuO_2 or ZnO, which display intrinsic pH sensitivity due to protonation–deprotonation equilibria occurring at their surfaces [8]; and (iii) conductive polymers with a pH-dependent redox behaviour such as polyaniline or polypyrrole, whose protonation states modulate their electrochemical response [5]. Although these approaches have shown reliable performances, the majority of the reported electrodes are self-made sensors that require personnel to be trained on sensor modification protocols and electrode maintenance, thus limiting its applicability in a wider scale for routine analytical laboratories. Consequently, some authors have shifted their attention to simpler sensing strategies based on electrode materials that are already widely available in electrochemical platforms, such as carbon [9,10] and gold [11–13]. In these systems, pH sensitivity arises from intrinsic surface redox processes, eliminating the need for additional sensing layers or complex fabrication steps.

However, despite the existing studies demonstrating pH responsiveness, most published work has primarily focused on confirming the existence of pH-dependent electrochemical signals or on proof-of-concept sensing applications. Comparatively little attention has been devoted to assessing the factors that ultimately determine the suitability of these systems for routine analytical use. In particular, the influence of electrode history and previous electrochemical treatments on the pH response, the effectiveness of surface regeneration strategies to restore analytical performance, and the quantitative impact of matrix components, especially ionic strength and chloride concentration, have not been systematically investigated for commercial SPEs. As a result, the robustness and reliability of these sensors under practical operating conditions remain insufficiently understood. Furthermore, critical analytical parameters such as repeatability, reversibility, inter-electrode reproducibility, surface conditioning protocols, long-term stability and matrix-dependent effects have received limited attention, despite their direct influence on measurement performance.

This limitation is particularly relevant for commercial SPEs, whose manufacturing process, surface heterogeneity and batch-to-batch variability may significantly influence

sensor performance in real-world applications. In the case of screen-printed gold electrodes (SPAuEs), these challenges may be further amplified by the complex composition of commercial gold inks, which contain metallic particles, binders and other additives that generate heterogeneous surfaces substantially different from those of conventional bulk gold electrodes. In addition, the screen-printing process may produce surface defects, heterogeneous gold particle distribution and variations in surface roughness that can affect electrochemical behaviour. Such characteristics may influence oxide formation and reduction processes, contribute to pre-treatment-dependent responses and anomalous calibration behaviour, and ultimately affect the analytical performance of voltammetric pH measurements.

Therefore, the objective of this work is to establish whether commercially available screen-printed electrodes can be reliably implemented as voltammetric pH sensors in routine analytical laboratories. To this end, a systematic evaluation of screen-printed carbon electrodes (SPCEs) and SPAuEs was conducted under conditions that mimic practical use, including repeated measurements, surface ageing, sensor-to-sensor variability, electrochemical regeneration procedures and matrix-dependent interferences. In contrast with previous studies that primarily focused on demonstrating pH responsiveness, the present work focuses on evaluating the factors that determine whether such responses can be translated into reliable analytical measurements. Beyond assessing analytical figures of merit, this study aims to define the operational boundaries, practical requirements and limitations governing the reliable use of commercial SPEs for pH determination.

2. Materials and Methods

2.1. Chemicals

Catechol was acquired from Fluka (Buchs, Switzerland) and dopamine and hydroquinone were supplied by Sigma-Aldrich (Steinheim, Germany). Other common chemical reagents including hydrochloric acid, sulfuric acid, acetic acid, boric acid, phosphoric acid, and potassium hydroxide were obtained from Merck (Darmstadt, Germany). All reagents were of analytical grade and all solutions were prepared using Milli-Q water (reference A+, Millipore, Molsheim, France).

Britton–Robinson buffers (BRB) were prepared by mixing 5 mL of acetic acid, phosphoric acid and boric acid, all of them at a concentration of 0.4 mol L^{-1}. Then, the pH was adjusted to the desired value by adding 1 mol L^{-1} KOH and the solution was further diluted to 50 mL.

2.2. Electrochemical Measurements

Electrochemical measurements were performed using an IviumStat2.h potentiostat (Ivium Technologies, Eindhoven, The Netherlands) controlled by the software IviumSoft (version 4.1217), also from Ivium Technologies. Screen-printed carbon electrodes (SPCE, ref. C110) and screen-printed gold electrodes (SPAuE, ref. C220AT) with 4 mm diameter were acquired from Methrom-Dropsens (Oviedo, Spain), and connected to the potentiostat by means of a flexible cable (ref CAC, Metrohm-Dropsens, Oviedo, Spain). All electrochemical measurements were performed using the full electrochemical cell provided by the SPE (including working electrode, pseudo-reference electrode, and counter electrode), at room temperature and without deaeration.

2.3. Screen-Printed Carbon-Based Electrodes

SPCEs were activated by performing cyclic voltammetric (CV) scans in NaOH. Unless otherwise stated, the activation was performed with 1 mol L^{-1} NaOH and using 20 cycles from 0 to +2 V at 100 mV s^{-1}.

Activated SPCEs were further modified by electrochemical cycling in dopamine, catechol or hydroquinone solutions using CV. In all cases, a 10 mmol L^{-1} solution of the desired modifier was prepared in BRB pH 7 and 5 CV cycles were carried out at 100 mV s^{-1}. The considered potential windows were from −0.5 V to +1.5 V for dopamine and from −0.8 V to +0.1 V for catechol and hydroquinone. Modified electrodes were soaked in 0.1 mol L^{-1} HCl to remove non-immobilized molecules from the surface prior to any electrochemical measurement.

CV measurements of pH employing SPCEs were performed by immersing the electrode in fresh BRB solutions with pH ranging from 2 to 10. Then, the potential was scanned from −0.4 V to +0.6 V at 50 mV s^{-1} and with a potential step of 5 mV. The electrode surface was cleaned between measurements by rinsing the electrode with 0.1 mol L^{-1} HCl.

2.4. Screen-Printed Gold-Based Electrodes

SPAuEs were activated by immersing the electrode in 0.1 M HCl for 10 min.

CV measurements of pH employing SPAuEs were performed by immersing the electrode in fresh BRB solutions with pH ranging from 2 to 12. Then, the potential was scanned from −0.4 V to +1.2 V at 700 mV s^{-1} and with a potential step of 5 mV. The electrode surface was cleaned after each calibration curve by applying 20 cyclic voltammograms from −0.4 V to +1.2 V at 700 mV s^{-1} in a pH 2 BRB.

3. Results and Discussion

3.1. Screen-Printed Carbon-Based Electrodes

SPCEs, in their commercially acquired form, were first analyzed by CV from −0.4 V to +0.6 V at different pH values ranging from 2 to 12 to characterise the electrode surface. No voltammetric signals were observed, thus indicating that commercial SPCEs do not present any intrinsic pH-responsive functional groups that can be easily oxidized or reduced. This finding differs from previous studies with other type of carbon electrodes, in which freshly polished glassy carbon electrodes [9] and edge-plane pyrolytic graphite electrodes [10] did provide intrinsic voltammetric signals attributed to surface quinone groups. Nevertheless, taking into account that the fabrication process of SPCEs involves carbon inks mixed with non-conductive materials such as organic solvents, binding pastes and additives [14], it is plausible that these materials partially block or mask the electroactive sites of the carbon surface. For this reason, electrochemical activation of the carbon surface was explored as a strategy to recover or enhance the intrinsic electroactivity of the electrode. This activation procedure has been widely employed to enhance electron-transfer properties and increase the active surface area as it introduces oxygen functional groups, results in a higher defect density, and induces the formation of nanostructures [15]. Following a simple activation of 5 cycles from 0 to +2 V at 100 mV s^{-1} in 0.1 mol L^{-1} NaOH, a voltammetric peak could be observed at pH 2 at ca. +0.1 V, thus confirming the introduction of oxidable oxygen functional groups. Nevertheless, this peak was only visible at pH 2 and 3 and showed poor stability, with a rapid decrease in current intensity for consecutive cycles that did not allow its use for repetitive measurements.

Given this lack of robustness, together with the fact that the response is confined to a very narrow acidic pH range, the use of commercial SPCEs as pH sensors necessarily relies on the extrinsic introduction of pH-sensing materials onto the electrode surface. A fast and reproducible strategy for electrode surface modification is the electrochemical deposition of redox-active organic layers. Building on this approach, Figure 1a–c display the voltammetric responses obtained at different pH values in monomer-free solutions using SPCEs modified by electrochemical cycling in dopamine, catechol and hydroquinone solutions, three structurally related molecules that exhibit a pH-dependent electrochemical behaviour.

In all cases, predominant voltammetric peaks associated with the quinone/hydroquinone redox conversion of the dihydroxybenzene moieties could be observed. In the case of catechol, a second redox process at more negative potential values was observed, which is consistent with other works reported in the literature [16]. As observed in Figure 1d, the introduction of these groups onto the SPCE surface provided a clear response to pH, with an oxidation peak shift consistent with an oxidation process involving 2 protons and 2 electrons, albeit slightly sub-Nernstian (slope values of 43.7 mV, 38.6 mV, and 37.2 mV for dopamine, catechol and hydroquinone, respectively). Nevertheless, Figure 1a–c also display a decrease in current intensity at higher pH values, which is not only related to pH but also to the number of measurements performed with the same electrode unit. This point was further demonstrated by remeasuring pH 2 after recording a single calibration curve. Taking hydroquinone as reference, in the second measurement of pH 2, the signal decreased to 52% of the original signal. When comparing these results with previous works reported in the literature, and taking dopamine as an example, this behaviour was also observed when dopamine was electropolymerized onto SPCE [17] or onto a GCE modified with carbon nanoallotropes [18], but not onto freshly polished GCE [19]. This suggests that the non-crystalline structure of carbon in SPCEs hinders the formation of stable electrochemically deposited layers, which in turn limits their long-term stability. As a consequence, careful optimization of the deposition conditions should be carried out to obtain sensors with sustained performance over repeated measurements. Taken together, these limitations make evident a significant drawback when considering commercial SPCEs as suitable substrates for robust pH sensing. Nevertheless, alternative SPE substrates may offer more favourable surface properties, potentially enabling more reliable platforms for pH sensing.

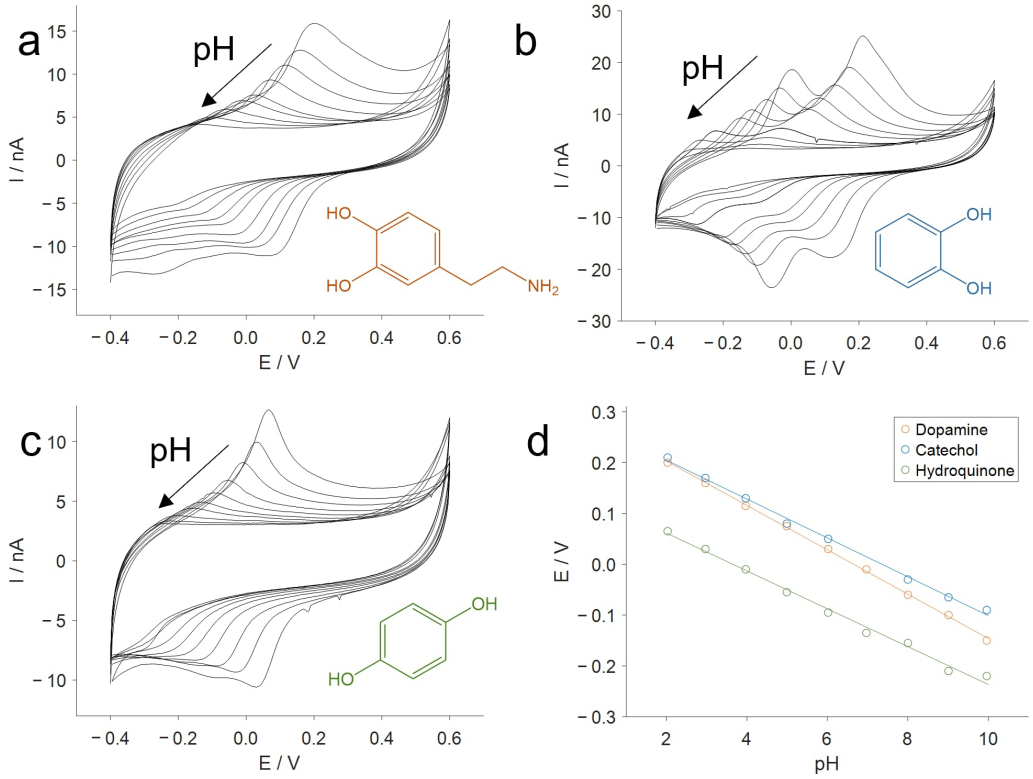


Figure 1. (**a**–**c**) CVs obtained for a pH range between 2 and 10 employing SPCEs activated with NaOH 1 mol L^{-1} and further modified with (**a**) dopamine, (**b**) catechol, and (**c**) hydroquinone. (**d**) Corresponding calibration curves.

3.2. Screen-Printed Gold-Based Electrodes

3.2.1. Voltammetric Optimization

Gold was then evaluated as the second most common material employed for SPEs. Gold electrodes are known to provide a pH response due to the formation of gold oxide at positive potentials (typically above 1 V), which is subsequently reduced during the reverse scan, giving rise to a pH-sensitive reduction peak. Although this process may be quite complex, a simplified proton-coupled electron-transfer reaction for this process in acid and alkaline media is displayed in Equations (1) and (2), respectively [13,20].

$$Au_2O_3 + 6H^+ + 6e^- \rightleftarrows 2Au + 3H_2O \quad (1)$$

$$AuOH + H^+ + e^- \rightleftarrows Au + H_2O \quad (2)$$

Thus, the first parameter examined was the width of the potential window, as this proved decisive for obtaining reproducible and well-defined reduction peak intensities with the SPAuE electrode. In this context, the system exhibited a strong dependence on the anodic limit, in line with the formation of gold oxides at positive potentials and their subsequent reduction during the reverse scan. Testing potential windows that restricted the anodic limit to 1.0 and 1.2 V revealed a clear advantage for the higher value, as applying 1.2 V produced a much better defined and more intense reduction peak across the pH range. In contrast, when the anodic limit was restricted to 1.0 V, the reduction peak intensity decreased noticeably, indicating that oxide formation was insufficient. As shown in Figure 2a, the improvement obtained at 1.2 V was more pronounced under basic conditions than under acidic ones. Moreover, a shift in the reduction peak toward more negative potentials was observed, particularly at low pH, whereas this shift was almost negligible at high pH. This trend may be attributed to the key role of protons in the reduction process (Equation (1)), but also to the fact that oxide formation occurs at more positive potentials under acidic conditions. Consequently, the smaller potential gap between oxide formation and the anodic limit at low pH, together with the higher proton availability in acidic media, provides a plausible explanation for the distinct reduction-peak behaviour observed under acidic and basic conditions. It is also worth noting that anodic limits higher than 1.2 V were not considered, as the peaks obtained at 1.2 V were already sufficiently well-defined across the pH range 2–12, and at basic pH the increase in oxidative intensity at this potential was already very pronounced.

Another key parameter to be optimized was the scan rate. In the context of voltammetric pH measurements under dynamic conditions, rapid acquisition is particularly important to maximise the number of measurements obtained in the shortest possible time. To evaluate the influence of this parameter, measurements were performed using four scan rates: 50, 200, 700 and 1000 mV s^{-1}. Figure 2b shows the response obtained for three representative pH values (3, 6 and 9) using a SPAuE at the different scan rates. As observed, increasing the scan rate led to a progressive enhancement in the current of the reduction peak, a behaviour attributable to the higher charge flux per unit time at faster scans due to a steeper diffusion layer, which translates into a higher-intensity peak. However, this increase in height comes at the expense of peak broadening and partial overlap between neighbouring peaks, which hinders the discrimination between pH values that are close to each other. A compromise between measurement speed and resolution was therefore required. Based on this criterion, a scan rate of 700 mV s^{-1} was selected, as it provided sufficiently rapid measurements while maintaining adequate separation between peaks corresponding to adjacent pH values. Under these conditions, the cathodic limit was set to −0.4 V, ensuring proper observation of all reduction signals within the pH range 2–12.

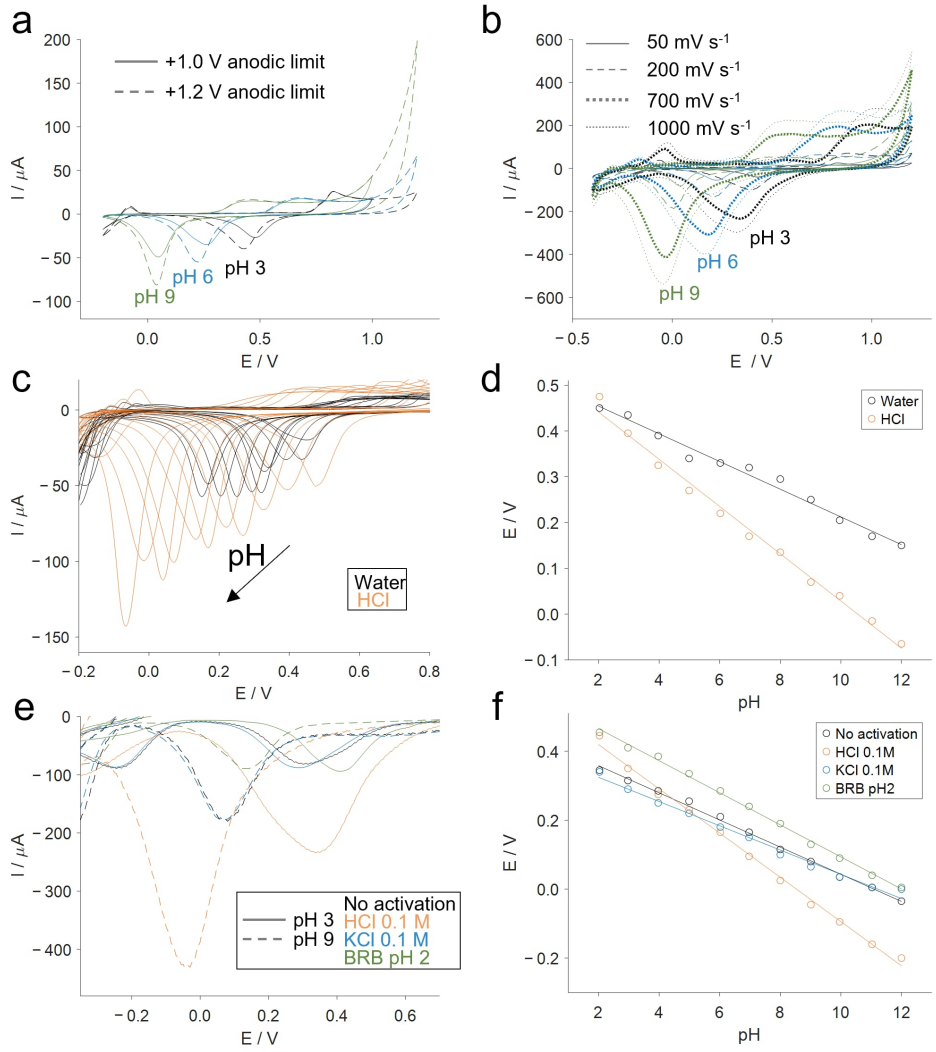


Figure 2. (**a**) Optimization of anodic limit with a fixed scan rate of 50 mV s^{-1}; and (**b**) optimization of scan rate using a fixed anodic limit of +1.2 V at three different pH values: pH 3 (black), pH 6 (blue) and pH 9 (green). (**c**,**d**) CVs and corresponding calibration curves obtained for a pH range between 2 and 12 employing untreated SPAuEs with intermediate cleaning using water or 0.1 M HCl. (**e**,**f**) CVs obtained at pH 3 and pH 9, and corresponding calibration curves obtained for a pH range between 2 and 12 employing SPAuEs pretreated for 10 min in different solutions. All measurements in (**c**–**f**) were performed at 700 mV s^{-1} and with a potential window between −0.4 and +1.2 V.

With these optimized parameters established, it is also important to consider that the formation of gold oxide (Equations (1) and (2)) is typically affected by the structure of gold, as well as the composition and state of charge of the involved oxyspecies [21]. Thus, the redox behaviour of solid gold electrodes cannot be directly extrapolated to SPAuEs. Taking this into account, CV measurements were performed using a SPAuE in BRB buffers with pH ranging from 2 to 12. As observed in Figure 2c,d (black signal), using the optimized CV measurement conditions, the reduction peak gradually shifted to more negative potentials as pH increases but the shift was not fully linear (R^2 = 0.983) and the slope was clearly sub-Nernstian, with a value of 30.3 mV, in contrast to the frequent super-Nernstian response observed for gold electrodes [21]. Both aspects, as well as signal intensity, improved when the SPAuE was rinsed with 0.1 mol L^{-1} HCl instead of water between measurements (Figure 2c,d, orange signal), yielding a slope of 51.6 mV, closer to the Nernstian value. This fact indicates an important role of HCl in the pH voltammetric response of SPAuEs, which may be related to either partial dissolution of the outermost gold layer and/or the

removal of inorganic species, mainly oxides, derived from the printing process. Thus, a pretreatment step consisting of immersing the electrode in 0.1 mol L^{-1} HCl for 10 min prior to any voltammetric measurement was added. As observed in Figure 2e,f, the pretreatment with HCl produced a similar effect to intermediate cleaning, with SPAuE pretreated with HCl giving rise to more intense peak, improved linearity and, in this case, super-Nernstian response (a slope of 64.2 mV). The observed slope exceeds the theoretical value expected for the formal Au_2O_3/Au equilibrium, which suggests that the electrochemical signal is likely generated by a more complex distribution of gold oxide species than those represented by Equations (1) and (2) [21,22]. In order to further understand the role of HCl, the same experiment was conducted by pretreating the electrode with 0.1 mol L^{-1} KCl and BRB buffer pH 2 (blue and green signals in Figure 2e–f, respectively). KCl did not improve the response compared to the untreated electrode, suggesting that chloride ions alone are insufficient to activate the surface. The enhanced performance observed after HCl treatment is consistent with acid-induced modifications of the surface oxide layer, although the exact mechanism cannot be established from the present data. However, the results obtained with BRB pH 2 indicate that the presence of protons alone is insufficient to successfully improve the pH response of SPAuEs. Once oxide species have been removed, the interaction of gold with the specific anions present in the pretreatment solution will also influence both peak size and position, with chloride producing a significantly larger activation effect than the phosphate, acetate and borate mixture present in BRB pH 2. One possible explanation is the formation of soluble Au(III) chlorocomplexes, which may alter the composition and structure of the surface oxide layer. Thus, unless otherwise stated, all subsequent CV measurements were performed using an SPAuE with a potential window of −0.4 to 1.2 V and a scan rate of 700 mV s^{-1}, and immersing the electrode in 0.1 mol L^{-1} HCl for 10 min prior to any CV measurement.

3.2.2. Analytical Performance Assessment

Once the CV experimental conditions were optimized, calibration curves were obtained at increasing pH values using BRB solutions ranging from pH 2 to 12 and employing a single SPAuE for all the measurements. Figure 3a shows representative CV voltammograms recorded with the SPAuE. The voltammograms exhibit well defined cathodic peaks that shift progressively towards more negative potentials as the pH increases (i.e., under more basic conditions), confirming a clear dependence of the voltammetric response of the SPAuE on the solution pH. It is important to note that these cathodic peaks are attributed to the reduction of gold oxides formed at positive potentials under acidic conditions, which participate in proton-coupled electron transfer processes and therefore display a potential shift consistent with the proton activity of the medium. Figure 3b (left) displays the corresponding calibration plot, constructed from eight independent calibration curves covering the full pH range. These calibration plots reveal a strong linear relationship between the reduction peak potential and the pH value across the entire studied range (pH 2–12), yielding a slope of approximately −63.7 mV, a value that can be associated with a super-Nernstian response of the system. This behaviour further confirms the sensitivity of the SPAuE towards proton-dependent redox processes and highlights its suitability for pH monitoring over a wide acidity range. In order to confirm that the observed potential shifts originate primarily from the gold working electrode, control calibration curves were recorded in triplicate using an external Ag/AgCl (3M) reference electrode. A strong linear relationship between the reduction peak potential and the pH value was also observed with a slope of −72.2 ± 0.4 mV, thus confirming the role of Au in the pH-response obtained.

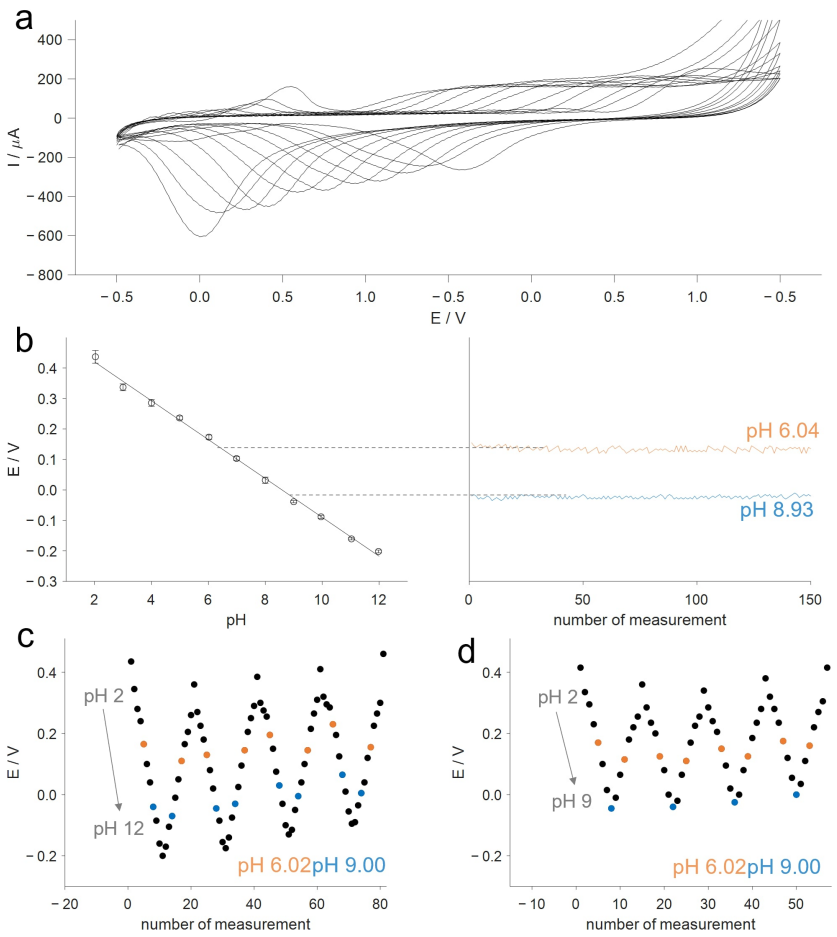


Figure 3. (**a**) Representative CV signals obtained with a SPAuE for a calibration curve in BRB buffers in the pH range 2–12. (**b**) Average calibration curve (left) obtained using 8 different SPAuE units and evolution of potential values (right) measured during 150 replicate measurements in two different solutions (pH 6.04 and 8.93). (**c**,**d**) Evolution of the potential measured during a reversibility study performed in the pH range 2–12 (**c**) and 2–9 (**d**). pH 6.02 and 9.00 are highlighted for clarification purposes.

The reproducibility and repeatability of the SPAuE were evaluated to assess the robustness of its voltammetric response. Reproducibility was determined as the relative standard deviation (RSD, %) of both the slope and the intercept obtained from eight independent calibration curves recorded using eight different SPAuE units. In contrast, repeatability was expressed as the RSD (%) of the slope and the intercept of the calibration plot calculated from eight consecutive calibration curves measured with the same SPAuE unit. The SPAuE exhibited excellent reproducibility (slope: 1.9%; intercept: 1.9%), indicating that the use of different sensor units does not affect the voltammetric determination of pH. However, the repeatability values were noticeably poorer (slope: 9.4%; intercept: 6.0%). This poorer repeatability is attributed to the intrinsic instability of the SPAuE during consecutive measurements at different pH values, which likely arises from the progressive modification of the gold surface, and suggests that the sensor's performance is influenced by the electrochemical history of the electrode. Because the calibration curves were recorded sequentially from acidic to strongly basic pH without intermediate reconditioning steps, the electrochemical history of the electrode accumulates over time. Gold oxide formation occurs at positive potentials under both acidic and basic conditions, but it is significantly more pronounced and stable in alkaline media [23]. As a result, the oxides generated at high pH are not fully reduced during the reverse scan, and these surface species persist

even when the medium becomes acidic again, leading to surface heterogeneity and signal drift. These cumulative surface changes ultimately result in higher RSD values for both the slope and the intercept.

The reversibility of the SPAuE was also evaluated (Figure 3c). To this end, a single SPAuE was used to record voltammetric measurements following two sequential pH sequences: first in ascending order (from pH 2 to pH 12) and subsequently in descending order (from pH 12 back to pH 2). From these measurements, eight calibration curves were constructed. The results show that the first calibration line progressively diverges from the subsequent ones, yielding RSD values of 7.7% for the slope and 7.0% for the intercept.

Following this first assessment, a second reversibility study was performed by restricting the pH window to a milder range (pH 2–9) in order to minimize the surface alterations associated with highly alkaline media (Figure 3d). Using the same SPAuE, eight additional calibration curves were obtained following ascending and descending pH sequences. In this case, the calculated RSD values were 6.9% for the slope and 7.5% for the intercept. Although the RSD values for the slope and intercept do not show a consistent quantitative improvement when the pH range is restricted from 2 to 12 to 2–9, the experimental data reveal a lower degree of signal drift during successive pH cycling. As illustrated in Figure 3d, the responses recorded at pH 6.02 and pH 9.00 remain clustered within a narrower potential interval (0.11 to 0.18 V for pH 6.02 and −0.05 to 0.00 V for pH 9.00) than those observed in the wider pH 2–12 study (0.11 to 0.23 V for pH 6.02 and −0.07 to 0.07 V for pH 9.00) displayed in Figure 3c, suggesting that the influence of electrode history is reduced when strongly alkaline conditions are avoided. Therefore, limiting the upper pH value to 9 appears to mitigate, although not completely eliminate, the influence of electrochemical history of the electrode on the voltammetric response. This behavior is consistent with the surface processes described above. In alkaline media, gold oxide formation is more extensive and produces more stable surface species, which are not fully reduced during the reverse scan. Because the return to acidic conditions occurs gradually, these species persist for several measurements, preventing the electrode from recovering its initial state. As a consequence, each new calibration curve is recorded on a surface that is slightly more modified than in the previous one, and the cumulative effect of moving stepwise from acidic to basic pH and back again leads to a progressive divergence from the initial calibration line. By limiting the upper pH limit to 9, the formation of these persistent oxide layers is mitigated, thereby helping preserve a more stable and reproducible SPAuE surface throughout consecutive measurements.

Taken together, repeatability and reversibility results indicate that, once the SPAuE has been exposed to highly basic conditions, a dedicated reconditioning step is required to restore its initial surface state. As discussed above, measurements in alkaline media promote the formation of stable gold-oxide species that are not removed during the single voltammetric scan performed at acidic pH. In view of this behavior, and to assess whether the progressive surface modification could be mitigated, the repeatability study was repeated but incorporating an intermediate regeneration stage between each of the eight calibration curves. Several regeneration strategies were tested including chemical rinsing with acid media, the application of a fixed potential in acid media and the performance of cyclic measurements in acid media. The best regeneration efficiency was obtained by introducing a cleaning step consisting of applying 20 cyclic voltammograms from −0.4 V to +1.2 V at 700 mV s^{-1} in a pH 2 BRB buffer prior to each new calibration line, with the aim of restoring a consistent SPAuE surface before each measurement and evaluating whether the intrinsic repeatability could be improved.

With the introduction of this regeneration step, the repeatability of the SPAuE improved noticeably: the RSD decreased to 5.2% for the slope and 4.7% for the intercept; these

values were substantially lower than those obtained without intermediate cleaning. These results confirm that the reconditioning step effectively stabilizes the electrode surface and mitigates the cumulative effects of prior measurements. Importantly, although the regeneration protocol requires 20 cyclic voltammetric scans, the complete procedure takes only approximately 1.5 min owing to the high scan rate employed (700 mV s^{-1}), thereby minimizing its impact on the practical implementation of the sensor, even in the case of online detection, for which a flow-injection analysis system could be introduced to alternate samples and reconditioning solution. Overall, these findings demonstrate that periodic surface regeneration is essential for maintaining consistent sensor performance and achieving improved intrinsic repeatability of the SPAuE.

The ability of the SPAuE to perform multiple consecutive measurements was subsequently evaluated. To assess this parameter, an initial calibration curve was recorded over the pH 2–12 range, followed by the regeneration step. The electrode was then immersed in test solutions of defined pH and subjected to 150 consecutive measurements (Figure 3, right). Two test solutions were used (pH 6.04 and pH 8.93), and in both cases the recorded potentials remained highly stable throughout the 150 scans. For the pH 6.04 solution, the standard deviation of the potential was 7.7 mV, while for pH 8.93 it was 5.1 mV, corresponding to variations within 0.12 and 0.08 pH units, respectively. These results confirm the excellent short-term stability of the SPAuE under repeated cycling.

In addition to stability, the accuracy of the SPAuE was also evaluated by calculating the relative error between the pH value obtained in the first of the 150 consecutive measurements and the reference pH determined with a glass electrode. The relative error was calculated from the absolute difference between the pH estimated with the SPAuE and the reference pH measured with the glass electrode, expressed as a percentage of the reference pH value. For the two test solutions (pH 6.04 and pH 8.93), the relative errors were 1.95% and 0.30%, respectively. These results indicate that the SPAuE provides an accurate initial pH estimate even before signal stabilization, confirming its suitability for rapid voltammetric pH screening.

To further assess the accuracy of the SPAuE under different chemical environments, its performance was evaluated using several buffer systems: acetate (pH 5.00), phosphate (pH 7.40), formate (pH 3.53), and maleate (pH 6.52), all prepared at three different concentrations (0.1, 0.05, and 0.01 mol L^{-1}). This approach allowed the examination of the influence of buffer ions and ionic strength on the sensor response. Using the calibration equations obtained from the standard calibration procedure, carried out, as usual, with BRB 0.1 mol L^{-1} solutions covering the pH 2–12 range, pH values were calculated from the recorded potentials and compared with the reference values through the relative error (%). Figure 4a provides a graphical comparison of the pH values obtained for the different buffer systems with those measured using the glass electrode. As Figure 4a shows, glass electrode is not especially sensitive to the ionic strength, apart from the fact that the real pH value slightly changes due to the influence of activity coefficients. The same happens for SPAuE at high salt concentrations, but there is an important effect at low ionic strengths. For the 0.1 mol L^{-1} buffers, the relative errors were 6.7% (acetate), 2.1% (phosphate), 3.0% (formate), and 5.3% (maleate). At 0.05 mol L^{-1}, the errors increased to 12.9%, 3.9%, 15.6%, and 2.5%, respectively, while at 0.01 mol L^{-1} they increased substantially to 52.9% (acetate), 12.3% (phosphate), 66.2% (formate), and 16.3%. Overall, these results indicate that the accuracy of the SPAuE is influenced far more by ionic strength than by the specific buffer system. Although acetate and phosphate share ions with the BRB solutions used for calibration, whereas formate and maleate do not, this difference does not appear to have a significant impact on performance. Instead, the sensor clearly performs better at buffer concentrations close to those used during calibration (0.1 mol L^{-1}), where the electrode response remains

more stable and less affected by variations in solution composition. In order to evaluate the influence of the pseudoreference electrode on the effect of the ionic strength, control experiments were carried out using an external Ag/AgCl (KCl 3 M) reference electrode. A similar trend was observed, yielding relative errors of 4.3%, 5.7% and 23.4% for acetate 0.1 mol L^{-1}, 0.05 mol L^{-1} and 0.01 mol L^{-1}, respectively. Thus, although some improvement can be gained by using a real reference electrode, significant errors were still observed at low values of ionic strength.

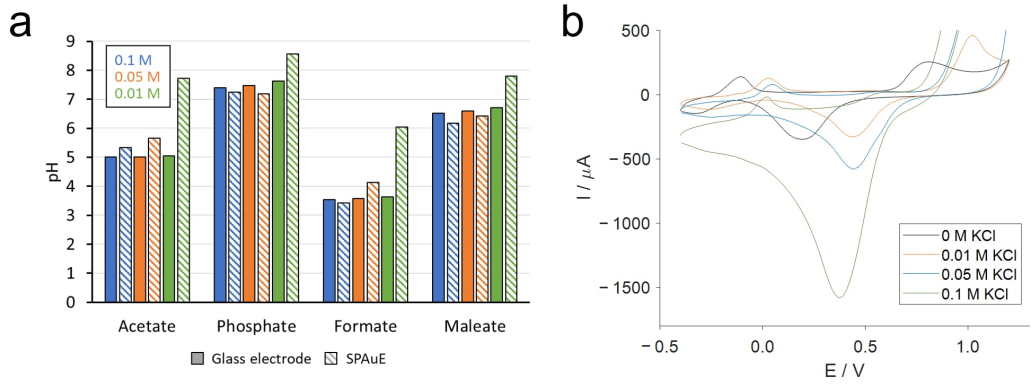


Figure 4. (**a**) Comparison between the pH values predicted by the SPAuE and those measured with the glass electrode for the different buffer systems (acetate, phosphate, formate, and maleate) prepared at three ionic strengths (0.1, 0.05, and 0.01 mol L^{-1}). (**b**) Cyclic voltammograms recorded in acetic–acetate buffer (0.1 mol L^{-1}) in the absence and presence of added chloride (0, 0.01, 0.05, and 0.1 mol L^{-1}).

A well-known limitation of gold-based sensors is their susceptibility to chloride interference, as chloride ions strongly adsorb onto the gold surface and promote the formation of Au–Cl surface complexes [22,24]. This interaction perturbs the interfacial structure and alters the kinetics of the redox process used for pH determination. To evaluate the impact of chloride ions, which were not included in the calibration, their effect on the SPAuE response was examined in a 0.1 mol L^{-1} acetic–acetate buffer by adding chloride at 0.01, 0.05, and 0.1 mol L^{-1}. As shown in Figure 4b, even the lowest chloride level tested (0.01 mol L^{-1}) had a clear effect on the voltammetric signal: the reduction peak shifted towards more positive potentials, while its intensity increased only slightly at this concentration. No further displacement of the peak potential occurred as the chloride concentration increased from 0.01 to 0.1 mol L^{-1}. In contrast, the peak magnitude continued to grow markedly with increasing chloride concentration, indicating that progressive chloride adsorption enhances the charge-transfer process associated with the reduction event. This behavior is consistent with the formation of surface chloride layers that stabilize specific gold oxidation states and facilitate electron transfer, thereby amplifying the reduction response without further altering its thermodynamic position. Nevertheless, it should be considered that the silver pseudo-reference electrode is also sensitive to the concentration of chloride due to the formation of AgCl on its surface, which could be an additional source of variation of the potential. In order to decouple the effect of each electrode, control experiments were carried out using an external Ag/AgCl (KCl 3M) reference electrode. The results showed a similar trend to the one displayed in Figure 4b, with the presence of KCl 0.01 M inducing shifts to more positive potential. However, when using an external reference electrode, the magnitude of this potential shift was better contained, with an overall shift of 90 mV instead of the 260 mV observed for the pseudoreference electrode. Therefore, the effect of chloride is indeed a combination of chloride interaction with both the Au working electrode and the Ag pseudoreference electrode.

Together, these results confirm that both ionic strength and chloride ions (even at low concentrations) have a significant influence on the SPAuE response and highlight the importance of controlling ionic strength and chloride levels in real samples when using gold electrodes for voltammetric pH sensing—even more so if a pseudoreference electrode is employed. Maintaining constant chloride concentrations and ionic strength in both calibration standards and samples may help to reduce variations arising from changes in the Ag pseudoreference potential as well as from matrix effects at the Au working electrode. In extreme situations, e.g., seawaters with high chloride levels and high ionic strengths, preliminary studies should be made to correct the pH calibration of the SPAuE unit (made with standard buffers) for the effect of the chloride concentration and the conductivity of the sample. As for the need to regenerate the electrode with 20 CVs between measurements after it has been exposed to alkaline media, this is not especially problematic in continuous flow monitoring, since the flows of the sample and the cleaning solution could be periodically alternated during the process.

4. Conclusions

This work provides a comparative assessment of commercial screen-printed electrodes for voltammetric pH sensing. The tested commercial SPCEs showed no intrinsic pH-responsive behavior, and although electrochemical activation or electrochemical surface modification could introduce pH-sensitive functionalities, the resulting signals were unstable and limited in range. These limitations, mainly associated with the non-crystalline nature of carbon inks, indicate that the employed SPCEs require substantial modification and optimization to perform reliably as pH sensors, which is not usually available in non-specialized analytical laboratories.

In contrast, the commercial SPAuEs tested exhibited a clear, robust and wide-range pH-dependent response based on the gold oxide/reduction process. Optimization of the voltammetric parameters (−0.4 to +1.2 V, 700 mV s^{-1}), together with an activation step consisting of immersing the electrode in 0.1 mol L^{-1} HCl prior to use, significantly improved sensitivity, linearity and peak definition, confirming the importance of proper surface conditioning for optimal performance. However, the sensor remained sensitive to its electrochemical history: sequential cycling from acidic to basic media led to the accumulation of stable gold-oxide species that were not fully removed at acidic pH, compromising both repeatability and reversibility. Introducing a reconditioning procedure (20 cyclic voltammograms from −0.4 V to +1.2 V at 700 mV s^{-1} in pH 2 BRB) effectively restored a consistent surface state, mitigated cumulative surface modifications, and markedly improved intrinsic repeatability.

The tested SPAuE demonstrated excellent short-term stability over 150 consecutive measurements and provided accurate initial pH estimates. Its accuracy, however, was strongly influenced by ionic strength. The lowest pH errors were obtained at 0.1 mol L^{-1}, whereas substantially larger errors were observed at lower ionic strengths, indicating that ionic strength had a greater effect on performance than the nature of the buffer system itself. In addition, chloride ions significantly affected the voltammetric response even at low concentrations. The effect of both chloride and ionic strength can be minimized but not completely removed by using a real Ag/AgCl electrode. These findings are consistent with previous studies using gold electrodes for pH determination based on the pH-dependent shift in the gold oxide reduction peak, but also highlight that the electrochemical response is strongly dependent on the nature and state of the gold surface. In the case of SPAuEs, the results presented here underline that factors such as surface conditioning, electrochemical history, and matrix composition critically govern the analytical performance and must be carefully controlled to ensure reliable measurements.

Overall, commercial SPAuEs represent a suitable and reliable voltammetric platform for pH screening across a wide range (pH 2–12), provided that appropriate pretreatment and periodic regeneration steps are implemented and that matrix effects (particularly ionic strength and chloride content) are properly controlled. Rather than focusing on the validation of a specific analytical application, the present study aims to critically assess the operational requirements, applicability and limitations of commercial SPEs for voltammetric pH sensing, thereby identifying key factors that must be considered before their implementation in complex real matrices.

Author Contributions: Conceptualization, C.P.-R., N.S. and J.M.D.-C.; formal analysis, C.P.-R., and N.S.; investigation, A.C., and L.I.; resources, N.S. and J.M.D.-C.; writing—original draft preparation, C.P.-R., and N.S.; writing—review and editing, A.C., L.I., C.P.-R., N.S. and J.M.D.-C.; visualization, C.P.-R., and N.S.; supervision, C.P.-R., N.S. and J.M.D.-C. All authors have read and agreed to the published version of the manuscript.

Funding: This work is supported by PID2022-136709OB-C22, which is funded by AEI/10.13039/501100011033/Unión Europea NextGenerationEU/PRTR and the Generalitat of Catalunya (Project 2021 SGR 00006).

Data Availability Statement: Data will be made available on request.

Conflicts of Interest: The authors declare no conflicts of interest.

References

1. Paul Shylendra, S.; Wajrak, M.; Kang, J.J. Advancements in Solid-State Metal pH Sensors: A Comprehensive Review of Metal Oxides and Nitrides for Enhanced Chemical Sensing: A Review. *IEEE Sens. J.* **2025**, *25*, 7886–7895. [CrossRef]
2. Vivaldi, F.; Salvo, P.; Poma, N.; Bonini, A.; Biagini, D.; Del Noce, L.; Melai, B.; Lisi, F.; Francesco, F.D. Recent Advances in Optical, Electrochemical and Field Effect pH Sensors. *Chemosensors* **2021**, *9*, 33. [CrossRef]
3. Tang, Y.; Zhong, L.; Wang, W.; He, Y.; Han, T.; Xu, L.; Mo, X.; Liu, Z.; Ma, Y.; Bao, Y.; et al. Recent Advances in Wearable Potentiometric pH Sensors. *Membranes* **2022**, *12*, 504. [CrossRef] [PubMed]
4. García-Guzmán, J.J.; Pérez-Ràfols, C.; Cuartero, M.; Crespo, G.A. Toward In Vivo Transdermal pH Sensing with a Validated Microneedle Membrane Electrode. *ACS Sens.* **2021**, *6*, 1129–1137. [CrossRef] [PubMed]
5. Ghoneim, M.T.; Nguyen, A.; Dereje, N.; Huang, J.; Moore, G.C.; Murzynowski, P.J.; Dagdeviren, C. Recent Progress in Electrochemical pH-Sensing Materials and Configurations for Biomedical Applications. *Chem. Rev.* **2019**, *119*, 5248–5297. [CrossRef] [PubMed]
6. Monteiro, M.C.O.; Koper, M.T.M. Measuring Local pH in Electrochemistry. *Curr. Opin. Electrochem.* **2021**, *25*, 100649. [CrossRef]
7. Xiao, W.; Dong, Q. The Recent Advances in Bulk and Microfluidic-Based pH Sensing and Its Applications. *Catalysts* **2022**, *12*, 1124. [CrossRef]
8. Manjakkal, L.; Szwagierczak, D.; Dahiya, R. Metal Oxides Based Electrochemical pH Sensors: Current Progress and Future Perspectives. *Prog. Mater. Sci.* **2020**, *109*, 100635. [CrossRef]
9. Lu, M.; Compton, R.G. Voltammetric pH Sensing Using Carbon Electrodes: Glassy Carbon Behaves Similarly to EPPG. *Analyst* **2014**, *139*, 4599–4605. [CrossRef] [PubMed]
10. Lu, M.; Compton, R.G. Voltammetric pH Sensor Based on an Edge Plane Pyrolytic Graphite Electrode. *Analyst* **2014**, *139*, 2397–2403. [CrossRef] [PubMed]
11. Kennedy, K.; Adib, M.R.; Rönnby, K.; Seymour, I.; Nolan, M.; O'Riordan, A. Gold/Gold Oxide as a Solid State on-Chip pH Sensing Probe for Food Applications. *Electrochim. Acta* **2026**, *567*, 148791. [CrossRef]
12. Li, L.; Limani, N.; Antony, R.P.; Dieckhöfer, S.; Santana Santos, C.; Schuhmann, W. Au Micro- and Nanoelectrodes as Local Voltammetric pH Sensors during Oxygen Evolution at Electrocatalyst-Modified Electrodes. *Small Sci.* **2024**, *4*, 2300283. [CrossRef] [PubMed]
13. Seymour, I.; O'Sullivan, B.; Lovera, P.; Rohan, J.F.; O'Riordan, A. Electrochemical Detection of Free-Chlorine in Water Samples Facilitated by in-Situ pH Control Using Interdigitated Microelectrodes. *Sens. Actuators B Chem.* **2020**, *325*, 128774. [CrossRef]
14. Suresh, R.R.; Lakshmanakumar, M.; Arockia Jayalatha, J.B.B.; Rajan, K.S.; Sethuraman, S.; Krishnan, U.M.; Rayappan, J.B.B. Fabrication of Screen-Printed Electrodes: Opportunities and Challenges. *J. Mater. Sci.* **2021**, *56*, 8951–9006. [CrossRef]

15. Jiménez-Pérez, R.; González-Sánchez, M.I.; Gomis-Berenguer, A.; Iniesta, J.; Valero, E. Enhanced Surface Properties and Electrochemical Performance of Carbon-Based Screen-Printed Electrodes via Hydrogen Peroxide Activation. *Electrochim. Acta* **2025**, *536*, 146721. [CrossRef]
16. Almeida, L.C.; Correia, R.D.; Palys, B.; Correia, J.P.; Viana, A.S. Comprehensive Study of the Electrochemical Growth and Physicochemical Properties of Polycatecholamines and Polycatechol. *Electrochim. Acta* **2021**, *386*, 138515. [CrossRef]
17. Algethami, F.K.; Rabti, A.; Mastouri, M.; Abdulkhair, B.Y.; Ben Aoun, S.; Raouafi, N. Highly Sensitive Capacitance-Based Nitrite Sensing Using Polydopamine/AuNPs-Modified Screen-Printed Carbon Electrode. *RSC Adv.* **2023**, *13*, 21336–21344. [CrossRef] [PubMed]
18. Zuaznabar-Gardona, J.C.; Fragoso, A. A Wide-Range Solid State Potentiometric pH Sensor Based on Poly-Dopamine Coated Carbon Nano-Onion Electrodes. *Sens. Actuators B Chem.* **2018**, *273*, 664–671. [CrossRef]
19. Amiri, M.; Amali, E.; Nematollahzadeh, A.; Salehniya, H. Poly-Dopamine Films: Voltammetric Sensor for pH Monitoring. *Sens. Actuators B Chem.* **2016**, *228*, 53–58. [CrossRef]
20. O'Sullivan, B.; Patella, B.; Daly, R.; Seymour, I.; Robinson, C.; Lovera, P.; Rohan, J.; Inguanta, R.; O'Riordan, A. A Simulation and Experimental Study of Electrochemical pH Control at Gold Interdigitated Electrode Arrays. *Electrochim. Acta* **2021**, *395*, 139113. [CrossRef]
21. Burke, L.D.; Nugen, P.F. The Electrochemistry of Gold: I. The Redox Behaviour of the Metal in Aqueous Media. *Gold Bull.* **1997**, *30*, 43–53. [CrossRef]
22. Kasian, O.; Kulyk, N.; Mingers, A.; Zeradjanin, A.R.; Mayrhofer, K.J.J.; Cherevko, S. Electrochemical Dissolution of Gold in Presence of Chloride and Bromide Traces Studied by On-Line Electrochemical Inductively Coupled Plasma Mass Spectrometry. *Electrochim. Acta* **2016**, *222*, 1056–1063. [CrossRef]
23. Burke, L.D.; O'Sullivan, J.F. The Stability of Hydrous Oxide Films on Gold. *J. Electroanal. Chem. Interfacial Electrochem.* **1990**, *285*, 195–207. [CrossRef]
24. Sibug-Torres, S.M.; Niihori, M.; Wyatt, E.; Arul, R.; Spiesshofer, N.; Jones, T.; Graham, D.; de Nijs, B.; Scherman, O.A.; Rao, R.R.; et al. Transient Au–Cl Adlayers Modulate the Surface Chemistry of Gold Nanoparticles during Redox Reactions. *Nat. Chem.* **2026**, *18*, 294–301. [CrossRef] [PubMed]

Disclaimer/Publisher's Note: The statements, opinions and data contained in all publications are solely those of the individual author(s) and contributor(s) and not of MDPI and/or the editor(s). MDPI and/or the editor(s) disclaim responsibility for any injury to people or property resulting from any ideas, methods, instructions or products referred to in the content.